A&A 586, A110 (2016)
DOI: 10.1051/0004-6361/201527460

Astronomy & Astrophysics

A study of the C_3H_2 isomers and isotopologues: first interstellar detection of HDCCC⋆

S. Spezzano[1,3], H. Gupta[2,⋆⋆], S. Brünken[3], C. A. Gottlieb[4], P. Caselli[1], K. M. Menten[5], H. S. P. Müller[3], L. Bizzocchi[1], P. Schilke[3], M. C. McCarthy[4], and S. Schlemmer[3]

[1] Max-Planck-Institut für extraterrestrische Physik, Giessenbachstr. 1, 85748 Garching, Germany
e-mail: spezzano@mpe.mpg.de
[2] California Institute of Technology, 770 S. Wilson Ave., M/C 100-22, Pasadena, CA 91125, USA
[3] I. Physikalisches Institut, Universität zu Köln, Zülpicher Str. 77, 50937 Köln, Germany
[4] Harvard-Smithsonian Center for Astrophysics, and School of Engineering & Applied Sciences, Harvard University, Cambridge, MA 02138, USA
[5] Max-Planck Institut für Radioastronomie, Auf dem Hügel 69, 53121 Bonn, Germany

Received 28 September 2015 / Accepted 12 November 2015

ABSTRACT

The partially deuterated linear isomer HDCCC of the ubiquitous cyclic carbene (c-C_3H_2) was observed in the starless cores TMC-1C and L1544 at 96.9 GHz, and a confirming line was observed in TMC-1 at 19.38 GHz. To aid the identification in these narrow line sources, four centimetre-wave rotational transitions (two in the previously reported $K_a = 0$ ladder and two new ones in the $K_a = 1$ ladder) and 23 transitions in the millimetre band between 96 and 272 GHz were measured in high-resolution laboratory spectra. Ten spectroscopic constants in a standard asymmetric top Hamiltonian allow the main transitions of astronomical interest in the $K_a \leq 3$ rotational ladders to be calculated to within 0.1 km s^{-1} in radial velocity up to 400 GHz. Conclusive identification of the two astronomical lines of HDCCC was provided by the V_{LSR}, which is the same as for the normal isotopic species (H_2CCC) in the three narrow line sources. In these sources, deuterium fractionation in singly substituted H_2CCC (HDCCC/$H_2CCC \sim 4-19\%$) is comparable to that in c-C_3H_2 (c-C_3H_2/c-$C_3HD \sim 5-17\%$) and similarly in doubly deuterated c-C_3H_2 (c-C_3D_2/c-$C_3HD \sim 3-17\%$), implying that the efficiency of the deuteration processes in the H_2CCC and c-C_3H_2 isomers are comparable in dark clouds.

Key words. astrochemistry – line: identification – ISM: molecules – ISM: clouds

1. Introduction

The study of deuterated molecules in the radio band yields constraints on the physical and chemical properties of the interstellar gas in the early stages of low-mass star formation (Caselli & Ceccarelli 2012). Cyclopropenylidene (c-C_3H_2) is one of the molecules frequently used in studies of deuterium fractionation in cold dark clouds, because lines of its rare isotopic species are relatively intense, the degree of fractionation is high, and c-C_3H_2 is believed to form solely by gas phase reactions (Gerin et al. 1987; Bell et al. 1988; Talbi & Herbst 2001; Turner 2001; Liszt et al. 2012; Spezzano et al. 2013). During recent observations of the doubly deuterated species c-C_3D_2 towards the starless cores TMC-1C and L1544, Spezzano et al. (2013) observed an unidentified line in the millimetre band that was tentatively assigned to the singly deuterated form of propadienylidene (H_2CCC)[1], a highly polar metastable carbene ($\mu = 4.17$ D) about 14 kcal mol^{-1} (7045 K) higher in energy than the more stable isomer c-C_3H_2 (Wu et al. 2010).

Propadienylidene (H_2CCC) was detected in space by Cernicharo et al. (1991) and Kawaguchi et al. (1991) shortly after its millimetre-wave rotational spectrum was measured in the laboratory (Vrtilek et al. 1990). Initially, it was observed towards the cold dark cloud TMC-1 in the centimetre and millimetre bands, and the carbon-rich asymptotic giant branch (AGB) star IRC+10216 in the millimetre band. Here, we report the detection of a line of HDCCC in the prestellar cores TMC-1C and L1544 in the millimetre band at 96.9 GHz and a confirming line in TMC-1 in the centimetre band at 19.38 GHz.

Although H_2CCC was first observed nearly 25 years ago in the laboratory and the interstellar gas, the deuterated species had not been observed in any astronomical source and the rotational spectrum of the partially deuterated species HDCCC had not been measured in the millimetre band prior to this work, but the two lowest transitions in the centimetre band had been measured earlier (Kim & Yamamoto 2005). In support of the astronomical identification of HDCCC and of future studies of the C_3H_2 isomeric system in the interstellar gas, the principal millimetre-wave rotational transitions of astronomical interest have now been measured in high resolution laboratory spectra.

⋆ Based on observations carried out with the IRAM 30 m Telescope. IRAM is supported by INSU/CNRS (France), MPG (Germany) and IGN (Spain).

⋆⋆ *Current address*: Division of Astronomical Sciences National Science Foundation, 4201 Wilson Boulevard, Suite 1045, Arlington, VA 22230, USA.

[1] Propadienylidene (Chemical Abstracts Services CAS #: 60731-10-4) is usually designated in the spectroscopic and astronomical literature as H_2CCC (e.g., Vrtilek et al. 1990; Cernicharo et al. 1991) to distinguish it from its cyclic isomer c-C_3H_2, and because it has a same structure and symmetry as the well known molecules formaldehyde (H_2CO) and ketene (H_2CCO). Although propadienylidene is occasionally designated as l-C_3H_2, here we follow the example of spectroscopists and astronomers and refer to propadienylidene as H_2CCC.

2. Laboratory and astronomical observations

2.1. Laboratory

Rotational lines of HDCCC were observed with the same 3 m long free-space double-pass absorption spectrometer used to measure the millimetre-wave spectrum of c-C_3D_2 (Spezzano et al. 2012). Guided by frequencies calculated with an effective rotational and centrifugal distortion constant derived from the two lowest transitions measured at centimetre wavelengths in a supersonic molecular beam (Kim & Yamamoto 2005), lines of HDCCC were observed in the millimetre band. Following optimization of the normal isotopic species (H_2CCC), the most intense lines of HDCCC were observed in a low pressure (~18 mTorr) DC discharge (140 mA) through a statistical mixture of deuterated acetylene (50% HCCD, 25% DCCD, and 25% HCCH), carbon monoxide (CO), and argon (Ar) in a molar ratio of 10:5:1, with the walls of the discharge cell cooled to 150 K. The acetylene sample was produced in real time by dropping an equal mixture of normal (H_2O) and heavy water (D_2O) on calcium carbide (CaC_2). Under these conditions, the signal-to-noise ratio (S/N) of lines of HDCCC near 160 GHz was ≥10 in 15 min of integration. In addition, the two lowest $K_a = 0$ lines in the centimetre band at 19 and 38 GHz reported earlier by Kim & Yamamoto (2005) were remeasured with the FT microwave spectrometer described in Spezzano et al. (2012), and the two $K_a = 1$ transitions ($2_{1,2}-1_{1,1}$ and $2_{1,1}-1_{1,0}$) were also measured.

In all, 27 rotational lines between 19 and 272 GHz with $J \leq 14$ and $K_a \leq 3$ (Table 1) are reproduced to an rms uncertainty (28 kHz) that is comparable to the measurement uncertainties with ten spectroscopic constants in Watson's S reduced Hamiltonian: three rotational constants, five fourth-order distortion constants (D_K was constrained to a theoretical value owing to the high correlation with A), and two sixth-order distortion constants (Table 2).

There is no evidence of deuterium hyperfine structure (hfs) when the fundamental transition of HDCCC is observed with high S/N at a resolution of 1 kHz in our molecular beam; therefore, no such structure should be present when this transition is observed in space. With these measurements, lines of HDCCC of principal astronomical interest in rotational ladders with $K_a \leq 3$ can now be predicted to an accuracy of about 0.1 km s^{-1} for transitions up to 400 GHz, allowing for precise measurements of HDCCC in the interstellar gas.

The evidence that HDCCC is the carrier of the lines observed in our laboratory discharge is overwhelming. The close harmonicity of nine lines in the $K_a = 0$ rotational ladder with similar relative intensities confirms that there are no misassignments. The derived rotational constants are in excellent agreement with those predicted from a benchmark empirical equilibrium structure of H_2CCC (Gauss & Stanton 1999), combined with theoretical vibration-rotation interaction constants in Wu et al. (2010). Specifically, the measured constants B and C are within 0.03% of those estimated from the theoretical structure, and the fourth-order distortion constants are within a factor of two of the corresponding constants in H_2CCC and within 20% of those that were calculated here at the B3LYP/cc-pVTZ level of theory and scaled by the ratio of the corresponding experimental (Gottlieb et al. 1993) and theoretical constants of the normal isotopic species H_2CCC. Additional evidence for this identification is provided by the relative intensities of lines of HDCCC that are the same to within 30% of those of H_2CCC under the same conditions, after taking the statistical mixture of the deuterated acetylene precursor into account.

Table 1. Laboratory frequencies of HDCCC.

$J'_{K'_a,K'_c} - J''_{K''_a,K''_c}$	Frequency (MHz)	Unc. (kHz)	O–C[a] (kHz)
$1_{0,1} - 0_{0,0}$	19 384.5098	2	0.5
$2_{1,2} - 1_{1,1}$	38 283.5891	2	−0.6
$2_{0,2} - 1_{0,1}$	38 768.0019	2	1.0
$2_{1,1} - 1_{1,0}$	39 251.4274	2	−0.1
$5_{0,5} - 4_{0,4}$	96 902.196	20	0.6
$6_{0,6} - 5_{0,5}$	116 271.438	20	−6.5
$7_{0,7} - 6_{0,6}$	135 634.586	20	−8.5
$8_{0,8} - 7_{0,7}$	154 990.661	20	26.6
$9_{0,9} - 8_{0,8}$	174 338.544	20	−13.6
$10_{0,10} - 9_{0,9}$	193 677.324	20	−40.1
$10_{1,9} - 9_{1,8}$	196 204.056	24	−15.1
$12_{1,12} - 11_{1,11}$	229 614.027	23	55.9
$12_{2,11} - 11_{2,10}$	232 512.813	20	−6.9
$12_{3,10} - 11_{3,9}$	232 544.540	21	57.5
$12_{3,9} - 11_{3,8}$	232 546.625	21	−34.7
$12_{2,10} - 11_{2,9}$	232 775.855	20	−6.1
$12_{1,11} - 11_{1,10}$	235 415.394	19	22.5
$13_{1,13} - 12_{1,12}$	248 731.752	19	−24.1
$13_{0,13} - 12_{0,12}$	251 629.269	20	32.3
$13_{2,12} - 12_{2,11}$	251 875.722	20	−15.2
$13_{3,10} - 12_{3,9}$	251 927.366	33	−42.7
$13_{1,12} - 12_{1,11}$	255 015.024	20	−28.7
$14_{1,14} - 13_{1,13}$	267 845.608	37	−56.7
$14_{2,13} - 13_{2,12}$	271 235.509	12	8.1
$14_{3,12} - 13_{3,11}$	271 303.986	41	41.2
$14_{3,11} - 13_{3,10}$	271 308.664	28	−29.1
$14_{2,12} - 13_{2,11}$	271 653.245	20	13.6

Notes. [a] Calculated with the spectroscopic constants in Table 2.

Table 2. Spectroscopic constants of HDCCC (in MHz).

Constant[a]	This work[b]	Expected[c]
A	199 370.(233)	199 755
B	9 934.225 82(81)	9 936.8
C	9 450.298 72(81)	9 452.8
D_K	15.95[d]	15.95
$D_{JK} \times 10^3$	353.89(50)	413.19
$D_J \times 10^3$	3.808 2(33)	3.79
$d_1 \times 10^6$	−256.62(164)	−235.43
$d_2 \times 10^6$	−91.00(250)	−107.81
$H_{KJ} \times 10^6$	−841.(59)	
$H_{JK} \times 10^6$	8.53(122)	

Notes. [a] Spectroscopic constants in Watson's S-reduced Hamiltonian in the I^r representation. [b] Numbers in parentheses are one standard deviation in units of the least significant digits. [c] Rotational constants calculated with the empirical equilibrium structure of Gauss & Stanton (1999) and the vibration-rotation interaction constants from Wu et al. (2010). The fourth-order centrifugal distortion constants were calculated at the B3LYP/cc-pVTZ level of theory and scaled by the ratio of the corresponding measured (Gottlieb et al. 1993) and theoretical constants of H_2CCC. [d] Constrained to the theoretical value.

Predictions based on this work will be available online via the Cologne Database for Molecular Spectroscopy[2] (Müller et al. 2005).

[2] http://cdms.de

Table 3. Observed line parameters of H_2CCC in TMC-1C and L1544.

Transition $J'_{K_aK_c} - J''_{K_aK_c}$	Frequency (GHz)	Ref.	E_{up} (cm^{-1})	T_{mb} (mK)	rms (mK)	W (K km s^{-1})	B_{eff} (%)	θ_{MB} ($''$)	$V_{LSR}{}^a$ (km s^{-1})	Δv^a (km s^{-1})	N^b ($\times 10^{10}$ cm^{-2})
TMC- 1C[c]											
$4_{14}-3_{13}$ (ortho)	82.395	1	6.18	70(9)	7	0.024(2)	81	30	5.98(1)	0.32(3)	27(1)
$4_{04}-3_{03}$ (para)	83.165	1	6.94	45(20)	6	0.011(2)	81	30	6.07(2)	0.2(1)	5.9(6)
$5_{15}-4_{14}$ (ortho)	102.992	1	9.62	57(10)	7	0.012(2)	80	25	5.97(1)	0.18(3)	25(2)
$5_{05}-4_{04}$ (para)	103.953	1	10.40	31(5)	3	0.007(1)	80	25	6.03(1)	0.21(2)	8.7(7)
L1544[d]											
$5_{15}-4_{14}$ (ortho)	102.992	1	9.62	69(8)	10	0.037(3)	80	25	7.11(2)	0.50(5)	83(4)
$5_{05}-4_{04}$ (para)	103.953	1	10.40	53(12)	10	0.024(4)	80	25	7.18(3)	0.42(7)	30(3)

Notes. [(a)] Derived from a least-squares fit of Gaussian profiles to the spectra in Figs. 1 and 2. [(b)] Calculated on the assumption that T_{ex} is 4 K. [(c)] Pointing position: $\alpha_{2000} = 04^h41^m16\overset{s}{.}1$, $\delta_{2000} = +25°49'43\overset{''}{.}8$. [(d)] Pointing position: $\alpha_{2000} = 05^h04^m17\overset{s}{.}21$, $\delta_{2000} = +25°10'42\overset{''}{.}8$.

References. (1) Vrtilek et al. (1990).

Table 4. Observed line parameters of HDCCC in TMC-1C and L1544.

Transition $J'_{K_aK_c} - J''_{K_aK_c}$	Frequency (GHz)	Ref.	E_{up} (cm^{-1})	T_{mb} (mK)	rms (mK)	W (K km s^{-1})	B_{eff} (%)	θ_{MB} ($''$)	$V_{LSR}{}^a$ (km s^{-1})	Δv^a (km s^{-1})	N^b ($\times 10^{9}$ cm^{-2})
TMC- 1C[c]											
$5_{05}-4_{04}$	96.902	1	9.70	17(4)	3	0.005(1)	80	27	6.09(2)	0.26(4)	64(7)
$7_{07}-6_{06}$	135.634	1	18.10	≤ 3	3	···	76	18	···	···	···
L1544[d]											
$5_{05}-4_{04}$	96.902	1	9.70	12(4)	3	0.005(1)	80	27	7.31(5)	0.41(1)	71(7)

Notes. [(a)] Derived from a least-squares fit of Gaussian profiles to the spectra in Figs. 1 and 2. [(b)] Calculated on the assumption that T_{ex} is 4 K. [(c)] Pointing position: $\alpha_{2000} = 04^h41^m16\overset{s}{.}1$, $\delta_{2000} = +25°49'43\overset{''}{.}8$. [(d)] Pointing position: $\alpha_{2000} = 05^h04^m17\overset{s}{.}21$, $\delta_{2000} = +25°10'42\overset{''}{.}8$.

References. (1) This work.

2.2. Astronomical

The millimetre-wave observations were done in several observing sessions between September 2012 and April 2014 with the IRAM 30 m telescope at Pico Veleta (Spain). The EMIR receivers in the E090 and E150 configuration were employed, and the observations were made by frequency switching with offsets of ±3.9 and ±7.8 MHz in the higher frequency band. All four EMIR sub-bands were connected to the FTS spectrometer, which was set to high resolution mode. The spectrum consisted of four 1.8 GHz wide sub-bands with 50 kHz channel spacing (corresponding to a velocity resolution of 0.15 km s^{-1} at 3 mm) and a total spectral coverage of 7.2 GHz. The $J_{K_aK_c} = 5_{05}-4_{04}$ transition of H_2CCC in TMC-1C was observed with VESPA with a frequency resolution of 20 KHz. Telescope pointing (checked about every two hours) was accurate to $3''-4''$. The coordinates (see Tables 3 and 4) for TMC-1C[3] are from Bell et al. (1988) and Gerin et al. (1987), and those of L1544 coincide with the peak of the 1.3 mm continuum dust emission from Ward-Thompson et al. (1999). The GILDAS[4] software (Pety et al. 2005) was used for the data processing.

Observations of the fundamental rotational transition of HDCCC near 19.4 GHz ($J_{K_aK_c} = 1_{01}-0_{00}$) were made in 2007 October during a search for a rotational line of the $CCCN^-$ anion[5] in TMC-1 (Thaddeus et al. 2008) with the NRAO 100 m Green Bank Telescope (GBT)[6]. The corresponding transition of H_2CCC near 20.8 GHz was also observed during the same session, but only for a fairly short time (~12 min vs. 12 h for HDCCC). The observing procedure was essentially the same as described in Brünken et al. (2007). The observations were done towards the Cyanopolyyne Peak of TMC-1 (see Table 5 for coordinates), and spectra were taken by position switching at a frequency resolution of 1.5 kHz across the 50 MHz band of the GBT spectrometer (other observing conditions were summarized in Thaddeus et al. 2008).

2.2.1. HDCCC

The $5_{0,5}-4_{0,4}$ transition of HDCCC at 96.9 GHz was observed in TMC-1C and L1544 (Figs. 1 and 2). Because the V_{LSR} is in excellent agreement with that of other molecules in these two narrow line sources, these spectra provide strong evidence that HDCCC has been observed for the first time in the interstellar gas. The probability of a misidentification due to a line of another carrier coinciding to within twice the typical line width of about 200 kHz is very small ($\sim 2 \times 10^{-3}$), owing to the very low density of lines in these two sources of about 20 lines in each 1.8 GHz wide sub-band. Additional evidence for an astronomical identification of HDCCC was sought by means of other transitions in the millimetre band; however, the rotational spectrum of HDCCC is not rich in lines. On the assumption that only levels in the $K_a = 0$ ladder are appreciably populated in these cold dense cores (those with $K_a \neq 0$ are not metastable and are

[3] The source referred to here as TMC-1C, following the nomenclature from Bell et al. (1988), is listed as JCMTSF J044115.2+254932 in the SIMBAD database (http://cds.u-strasbg.fr).

[4] http://www.iram.fr/IRAMFR/GILDAS

[5] The $J = 2-1$ transition of $CCCN^-$ is 22 MHz higher in frequency than the fundamental transition of HDCCC.

[6] The National Radio Astronomy Observatory is a facility of the National Science Foundation operated under cooperative agreement by Associated Universities, Inc.

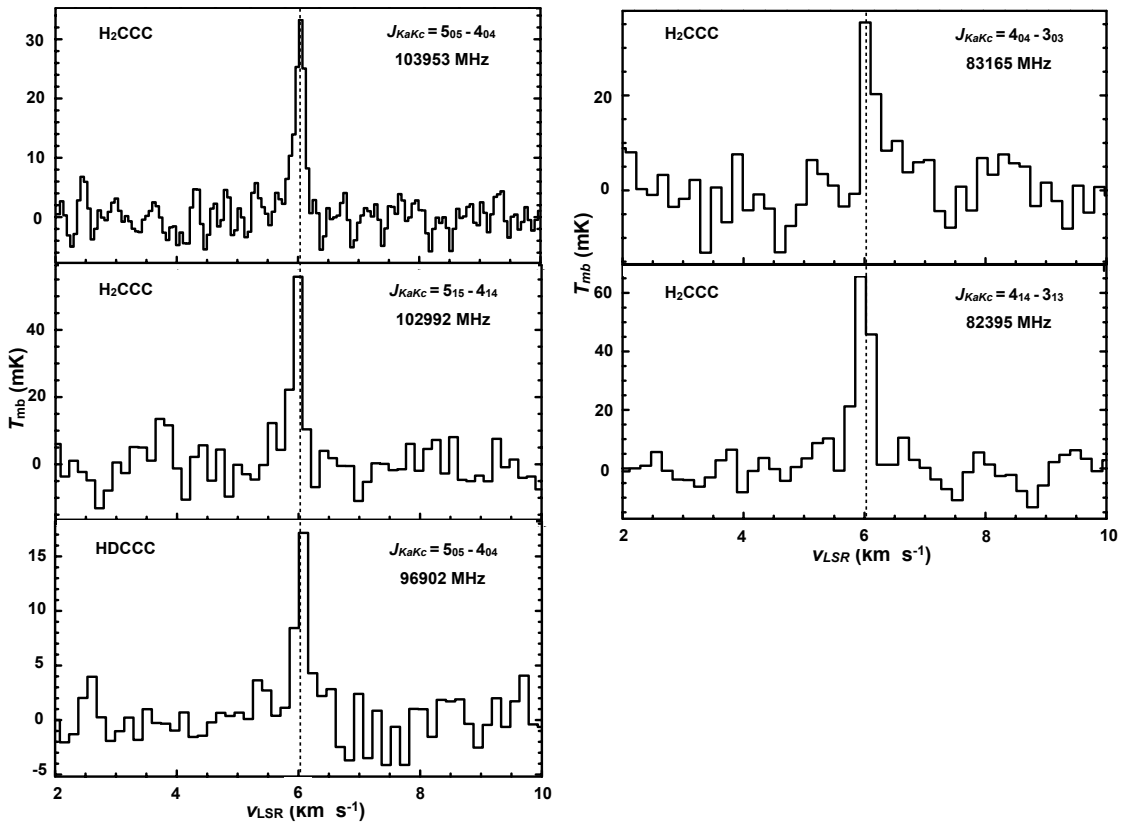

Fig. 1. Spectra of H_2CCC and HDCCC observed towards TMC-1C with the IRAM 30 m telescope. The integration times for H_2CCC were 3 h at 82 and 83 GHz, 4 h at 102 GHz, and 23 h at 103 GHz. For HDCCC the integration time was 16 h.

higher in energy by ≥12 K), there are three transitions that are readily accessible with current ground-based telescopes and that might be detectable with deep integrations: the two lowest ones at 19 and 38 GHz and one at 136 GHz.

Our initial attempt to detect a second line of HDCCC in the millimetre band was inconclusive. Although the transition at 135.6 GHz was not detected in TMC-1C with the IRAM 30 m telescope, our upper limit of the main beam temperature at this frequency (≤3 mK) is higher than predicted from the column density derived from the line at 96.9 GHz on the assumption that the excitation temperature is 4 K (see Sect. 3). We then realized that the $1_{0,1}-0_{0,0}$ transition at 19 GHz was covered in 2007 October in a deep search for the $CCCN^-$ anion in TMC-1 with the GBT (Thaddeus et al. 2008). Shown in Fig. 3 are the spectra with the fundamental transition of HDCCC and H_2CCC in TMC-1 at the precise V_{LSR} of 5.8 ± 0.1 km s^{-1} in this much studied position in the Taurus molecular cloud, confirming our initial assignment of the line at 96.9 GHz to the $5_{0,5}-4_{0,4}$ transition of HDCCC. As in the laboratory spectrum (Sect. 2.1), there is no evidence of deuterium hyperfine structure in the line in TMC-1 at 19 GHz.

2.2.2. H_2CCC

Simultaneous with the observations of HDCCC (Sect. 2.2.1), a para ($5_{0,5}-4_{0,4}$) and an ortho ($5_{1,5}-4_{1,4}$) transition of the main isotopic species H_2CCC were observed in TMC-1C and L1544 in 2012 September; and two additional transitions ($4_{0,4}-3_{0,3}$ and $4_{1,4}-3_{1,3}$) were observed in TMC-1C in 2014. The line parameters and derived column densities are reported in Table 3, and the spectra are shown in Figs. 1 and 2.

Owing to the two equivalent off-axis hydrogen atoms, H_2CCC has ortho and para symmetry states with a relative statistical weight (ortho/para) of 3:1, where rotational levels with odd K_a have ortho symmetry and those with even K_a have para symmetry. Monodeuterated HDCCC does not have ortho/para symmetry. It has been shown that the ortho/para ratio might depart from the statistical value, especially at the low temperatures that characterize cold dark cores, such as TMC-1C and L1544 (T = 4−10 K, Park et al. 2006). While analysing our data, we do not constrain the value of the ortho/para ratio, except in the case of TMC-1 where just one (para) line has been observed. In this case the ortho/para ratio was constrained to the statistical value (see Sect. 3).

3. Analysis

The column densities in Tables 3−5 were calculated with the following expression for optically thin transitions in rotational equilibrium at a temperature T_{ex} (Goldsmith & Langer 1999):

$$\frac{N_u}{g_u} = \frac{J(T_{ex})}{J(T_{ex}) - J(T_{bg})} \frac{3kW}{8\pi^3 \nu S \mu^2} = \frac{N}{Z} e^{\frac{E_u}{kT_{ex}}}, \quad (1)$$

where N_u, g_u, and E_u are the column density, degeneracy, and energy of the upper state of the transition; W is the integrated intensity; ν the frequency; S the rotational line strength; μ the dipole moment; Z the rotational partition function; and $J(T) \equiv \frac{h\nu}{k}(e^{\frac{h\nu}{kT}} - 1)^{-1}$. The factor $J(T_{ex})/[J(T_{ex}) - J(T_{bg})]$ accounts for the line absorption of the cosmic background radiation (T_{bg} = 2.7 K), and is significantly larger than unity at the low excitation temperatures (T_{ex} < 10 K) inferred for H_2CCC and other polar molecules in cold dark clouds. The column densities were calculated assuming an excitation temperature of 4 K,

Table 5. Centimetre-wave lines of HDCCC and H_2CCC in TMC-1.

Molecule	Transition $J'_{K_aK_c} - J''_{K_aK_c}$	Frequency (GHz)	Ref.	E_{up} (cm^{-1})	$T_A{}^a$ (mK)	W (K km s^{-1})	η_{MB} (%)	θ_{MB} ($''$)	$V_{LSR}{}^a$ (km s^{-1})	Δv^a (km s^{-1})	N^b (10^9 cm^{-2})
HDCCC	$1_{01} - 0_{00}$	19.384	1	0.647	13(3)	0.006(2)	0.880	37	5.62(3)	0.28(6)	118(36)
					10(6)				6.02(2)	0.14(11)	
H_2CCC (para)	$1_{01} - 0_{00}$	20.792	2	0.694	158(19)	0.054(18)	0.867	36	5.71(7)	0.28(4)	769(231)^c

Notes. Pointing position for TMC-1: $\alpha_{2000} = 04^h41^m42.49^s, \delta_{2000} = +25°41'26.9''$. Estimated 1σ uncertainties (in parentheses) are in units of the least significant digits. $^{(a)}$ Derived from a least-squares fit of Gaussian profiles to the spectra in Fig. 3. $^{(b)}$ Calculated on the assumption that $T_{ex} = 4$ K, the value derived for H_2CCC in TMC-1 by Kawaguchi et al. (1991). $^{(c)}$ For para H_2CCC. On the assumption that the ortho/para ratio is 3, N(ortho + para) = $3076(923) \times 10^9$ cm^{-2}.

References. (1) This work; (2) Vrtilek et al. (1990).

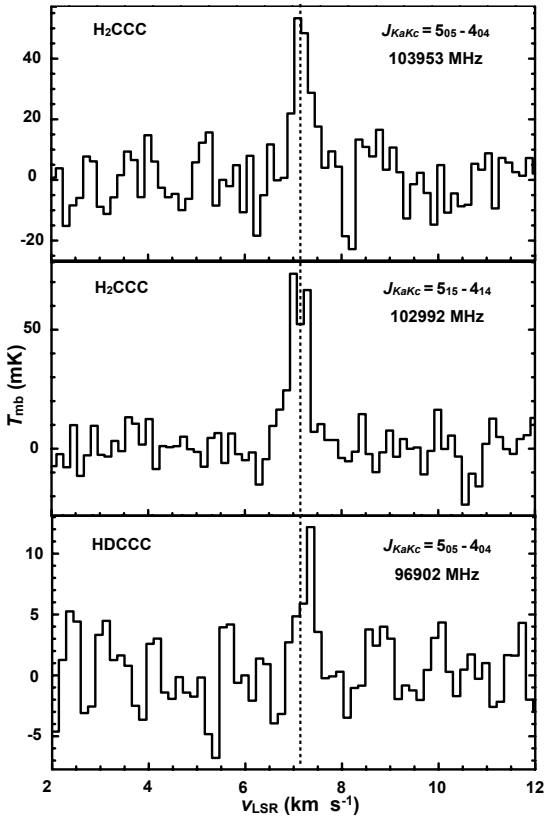

Fig. 2. Spectra of H_2CCC and HDCCC observed towards L1544 with the IRAM 30 m telescope. The integration times were 4 h for H_2CCC and 9.6 h for HDCCC.

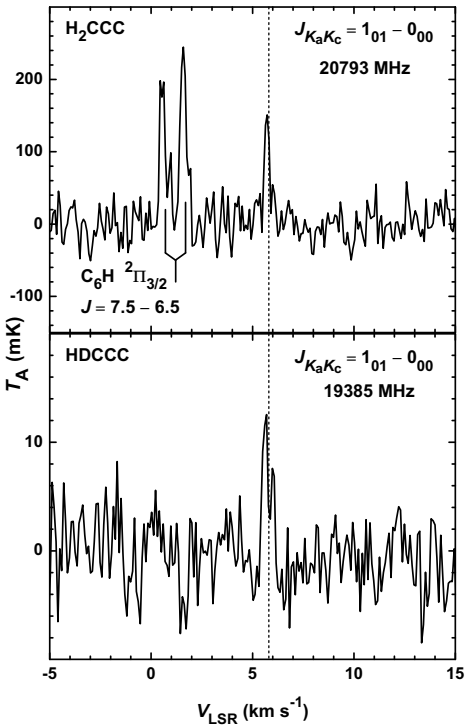

Fig. 3. Fundamental transitions of HDCCC and H_2CCC in TMC-1. Also present in the upper panel is the hyperfine-split transition of C_6H in the lower Λ component (e) at 20792.872 and 20792.945 MHz. Partially resolved kinematic structure is seen in the lines of HDCCC and C_6H, but not in H_2CCC owing to the lower S/N. The dashed line at +5.8 km s^{-1} indicates the systemic velocity of TMC-1. The integration time was approximately 11.5 h for the HDCCC and 12 min for the H_2CCC spectrum. Both spectra were Hanning-smoothed to a frequency resolution of 6.1 kHz. A similar spectrum was observed by Cernicharo et al. (1987), see Fig. 2 lower left panel in their paper, and Fossé et al. (2001), see Fig. 1 upper panel. In the paper by Cernicharo et al. (1987), the line of H_2CCC was reported as an unidentified feature because the laboratory spectrum of H_2CCC was not known yet.

by analogy with earlier work from Cernicharo et al. (1991) and Kawaguchi et al. (1991). On this assumption, from the column densities derived from the para and ortho lines of H_2CCC in TMC-1C and L1544, we infer ortho/para ratio of ∼3, which is consistent with the canonical ratio of 3. There are three principal sources of uncertainty in our derived column densities of H_2CCC and HDCCC: the excitation temperature, the ortho/para ratio in H_2CCC, and possible systematic uncertainties in the integrated areas of the observed line profiles. The results here allow us to derive the D/H ratio in H_2CCC in three sources for the first time. On the assumption that T_{ex} is 4 K in both H_2CCC and HDCCC, the D/H ratio in H_2CCC is 19 ± 5% in TMC-1C and 6 ± 1.3% in L1544 (Fig. 4). However, more observations are needed to better constrain the excitation temperature in both isotopic species and, in turn, the D/H ratio. Similarly, the centimetre-wave observation of the fundamental transition of HDCCC and para H_2CCC allowed us to estimate an approximate D/H ratio in TMC-1. We find that the extent of the deuteration in TMC-1 (4 ± 1.6%) is comparable to L1544, but is two-to-five times less than in TMC-1C.

3.1. Excitation and abundance of H_2CCC and HDCCC

To determine whether LTE is a good approximation for estimating the rotational excitation temperature (T_{ex}) and column density (N) of H_2CCC and HDCCC (Sect. 3), T_{ex} and N were compared with the corresponding properties of H_2CCC

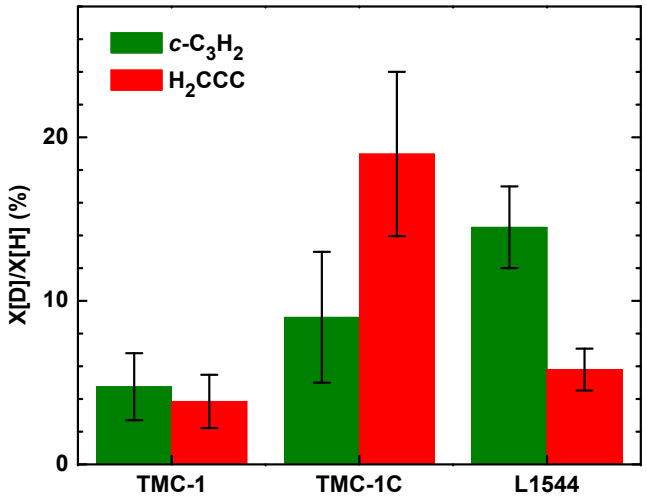

Fig. 4. D/H isotopic ratio in the carbene isomers H_2CCC and c-C_3H_2 in three dense cores in the Taurus molecular cloud: TMC-1, TMC-1C, and L1544. For c-C_3H_2, the heights of the bars indicate the average value, and the error bars the range of values inferred in previous studies of TMC-1 (Turner 2001) and of TMC-1C and L1544 (Spezzano et al. 2013).

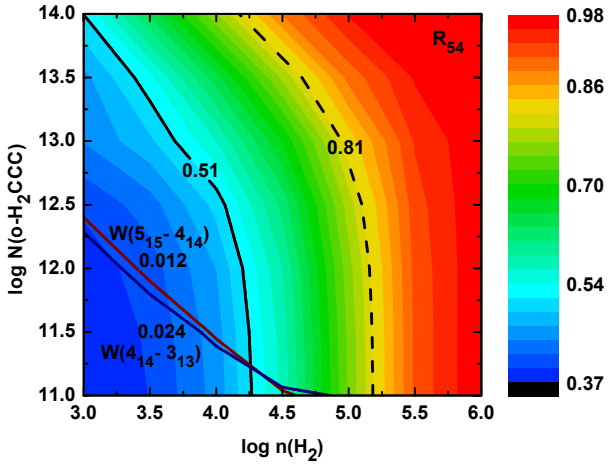

Fig. 5. Integrated area (W) for the $4_{1,4}$–$3_{1,3}$ transition (blue contour) and $5_{1,5}$–$4_{1,4}$ transition (red contour) of H_2CCC, and the ratio of the integrated areas R_{54} (solid black contour) versus the total column density of ortho H_2CCC and the H_2 density.

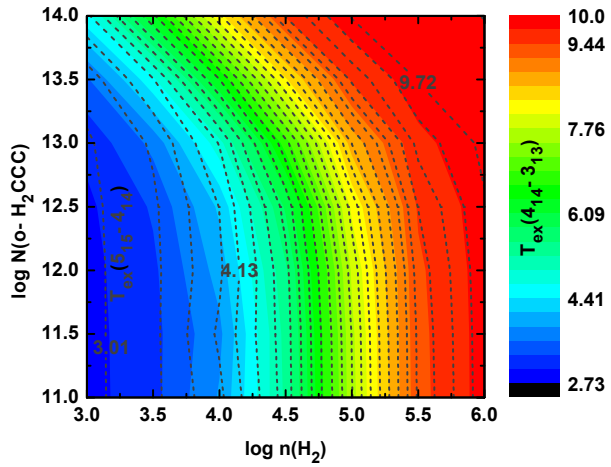

Fig. 6. Dependence of the excitation temperature (T_{ex}) of the $4_{1,4}$–$3_{1,3}$ and $5_{1,5}$–$4_{1,4}$ transitions of ortho H_2CCC on the column density and the H_2 density, on the assumption that the kinetic temperature is 10 K. The colour scale applies to the $4_{1,4}$–$3_{1,3}$ transition and the dashed contours to the $5_{1,5}$–$4_{1,4}$ transition.

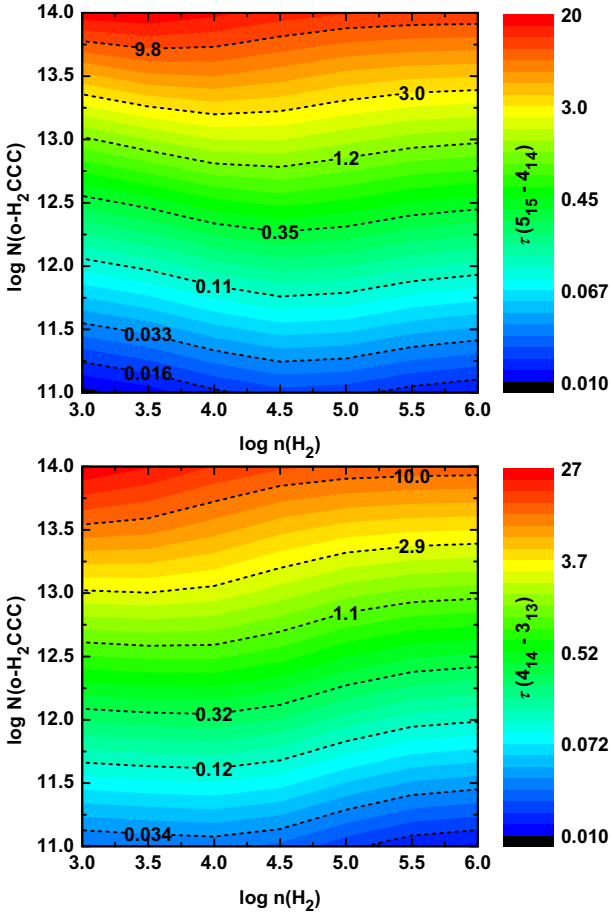

Fig. 7. Dependence of the optical depths (τ) of the $4_{1,4}$–$3_{1,3}$ and $5_{1,5}$–$4_{1,4}$ transitions of ortho H_2CCC on the column density and the H_2 density.

obtained from statistical equilibrium calculations with RADEX (van der Tak et al. 2007). The calculations were done for a uniform spherical geometry for TMC-1C, a line width of 0.3 km s^{-1} (FWHM), a kinetic temperature of 10 K, and a radiation temperature of 2.73 K. Following Cernicharo et al. (1999), we used collisional de-excitation rates that are two times higher than those for ortho-H_2CO with para H_2 as provided in the LAMDA database (Schöier et al. 2005; Wiesenfeld & Faure 2013). Only the lowest 18 rotational levels in the $K_a = 1$ ladder of H_2CCC were included, because the cross-ladder collisional rates ($\Delta K = 2$) are nearly an order of magnitude lower. Similarly, collisions with ortho-H_2 were neglected because the ortho/para ratio for H_2 is negligible at 10 K (cf., Troscompt et al. 2009).

Summarized in Figs. 5–7 are the results of the statistical equilibrium calculations. It is evident that the integrated areas (W) of the two ortho transitions of H_2CCC and the ratio of the two imply that $\log n(H_2) \sim 4.25$ and $\log N \sim 11.25$ (i.e., $n(H_2) = 2 \times 10^4$ cm^{-3} and $N = 2 \times 10^{11}$ cm^{-2}; Fig. 5). Under the same conditions we estimate that $T_{ex} \sim 4$ K (Fig. 6), and H_2CCC is optically thin in both transitions (i.e., $\tau \leq 0.05$ in $4_{1,4}$–$3_{1,3}$ and $5_{1,5}$–$4_{1,4}$; Fig. 7). As a result, we find that the rotational

Table 6. Column density and excitation temperature of ortho H_2CCC in TMC-1C.

Property	LTE	RADEX
$N(\mathrm{cm}^{-2})$	2.6×10^{11} [a]	1.8×10^{11}
T_{ex} (K)	4 [b]	4.6 [c]
T_{kinetic} (K)	···	10.0

Notes. [(a)] Average value of the column densities reported in Table 3 for ortho-H_2CCC in TMC-1C. [(b)] T_{ex} assumed by analogy with Cernicharo et al. (1991) and Kawaguchi et al. (1991). [(c)] Approximate mean of 4.4 K for the $5_{1,5}-4_{1,4}$ transition and 4.8 K for the $4_{1,4}-3_{1,3}$ transition at $\log n = 4.25$ and $\log N = 11.25$.

temperature derived for H_2CCC in TMC-1 by Cernicharo et al. (1991) and Kawaguchi et al. (1991) is valid for TMC-1C, hence also a valid assumption for L1544. We also find that the column density derived for ortho H_2CCC on the assumption of LTE is essentially the same as derived with RADEX (see Table 6).

4. Discussion

The present work is a preliminary study of different isomers and isotopologues of the C_3H_2 system. Isomers and isotopologues are precious tools for astrochemists because they convey useful information for disentangling different chemical routes that might correspond to different physical conditions. In particular, the astrophysically relevant properties of the C_3H_2 system studied in this paper are the D/H abundance ratio in each isomer and the cyclic-to-linear abundance ratio.

The cyclic-to-linear isomeric ratio of C_3H_2 appears to depend on the region where the isomers are observed, meaning that the c-C_3H_2/H_2CCC ratio increases with decreasing electron abundance (Fossé et al. 2001). A summary of the c-C_3H_2/H_2CCC ratio in different environments is reported in Table 7. In dense molecular clouds, the ratio is between 20 and 40 (Kawaguchi et al. 1991; Cernicharo et al. 1991; Fossé et al. 2001), while in diffuse clouds it is lower by one order of magnitude (Cernicharo et al. 1999). In the Horsehead nebula PDR, the c-C_3H_2/H_2CCC ratio has a value of three to five in the diffuse gas, and it increases by a factor of 4 when penetrating in the denser region of the cloud (Teyssier et al. 2005). Towards the Orion Bar a c-C_3H_2/H_2CCC ratio of 34 has been observed very recently (Cuadrado et al. 2015). Perhaps alternative formation/destruction routes occur towards the Orion Bar, which is a very extreme environment (>300 times the far-UV radiation flux with respect to the Horsehead nebula), which might allow endothermic reactions and reactions with a high energy barrier to become efficient. The c-C_3H_2/H_2CCC ratio in TMC-1C is about two times higher than in TMC-1, along the filament in TMC-1 (see Fig. 3 in Fossé et al. (2001), and in L1544. The causes for this behaviour might be a systematic error in the H_2CCC column density (see Sect. 3), the overall difficulty in deriving accurate column densities of c-C_3H_2, or different physical conditions in TMC-1C with respect to TMC-1 and L1544.

The variation in the cyclic-to-linear ratio in different environments is related to distinct destruction and possibly formation pathways for the two isomers. These pathways still need to be fully understood. Talbi et al. (2009) present the results of calculations on the dissociative recombination of cyclic and linear $C_3H_3^+$ with electrons. It is shown that the formation of c-C_3H_2 from c-$C_3H_3^+$ is more efficient than the formation of H_2CCC from l-$C_3H_3^+$. A similar result was obtained by Adams & Babcock (2005), who in fact observed in an afterglow experiment that the cyclic $C_3H_3^+$ recombines with electrons faster than the linear isomer. Interestingly, Chabot et al. (2013) show that with their new semiempirical model for calculating branching ratios while c-C_3H is the main product of the dissociative recombination of c-$C_3H_2^+$ with electrons, l-C_3H is not the main product of the recombination of l-$C_3H_2^+$ with electrons. Unfortunately, the branching ratios of the dissociative recombination of linear and cyclic $C_3H_3^+$ are not provided in Chabot et al. (2013).

The formation of c-C_3HD and c-C_3D_2 in dense cores has been studied for a long time (Gerin et al. 1987; Bell et al. 1988; Spezzano et al. 2013), and it is believed to occur through subsequent deuteration of c-C_3H_2 via reactions with H_2D^+, D_2H^+, and D_3^+ followed by the dissociative recombination of the ionic intermediate with electrons (see Fig. 3 in Spezzano et al. 2013). The intermediates of this reaction scheme are $C_3H_3^+$, $C_3H_2D^+$, $C_3HD_2^+$, and $C_3D_3^+$. When shown schematically, singly deuterated carbenes are produced by the formal reactions

$$RH_2 + H_2D^+ \rightarrow RH_2D^+ + H_2 \quad (2)$$

$$RH_2D^+ + e^- \rightarrow RHD + H \quad (3)$$

where $RH_2 \equiv c$-C_3H_2 (or H_2CCC), and the doubly deuterated carbenes by the reactions

$$RHD + H_2D^+ \rightarrow RHD_2^+ + H_2 \quad (4)$$

$$RHD_2^+ + e^- \rightarrow RD_2 + H. \quad (5)$$

For simplicity only the reactions with H_2D^+ are shown, but the same set of reactions will proceed with D_2H^+ and D_3^+. Table 7 and Fig. 4 report the D/H abundance ratios in both the cyclic and linear isomers of C_3H_2 in TMC-1C, L1544, and TMC-1. The D/H abundance ratio in both the cyclic and linear form of C_3H_2 are similar in all our observations, suggesting that the deuteration of the linear isomer might follow the same reaction scheme as the cyclic, with the difference that the deuteration of the linear isomer will not proceed as straightforwardly as the cyclic. In contrast to the cyclic, the linear deuterated intermediate ion (H_2CCCD^+) will have to undergo atom exchange or structural rearrangement while recombining with electrons, otherwise it will react back to H_2CCC. More experimental and theoretical studies are required to understand the detailed mechanism of deuteration of H_2CCC. TMC-1C shows an enhanced deuteration in the linear isomer compared to the cyclic. Given the difficulty in deriving accurate column densities for c-C_3H_2, and the possibility of having a systematic error in the column density derived for H_2CCC in TMC-1C, the authors do not feel the necessity to put too much emphasis on this result.

In dense prestellar and protostellar dark cloud cores, the c-C_3HD/c-C_3H_2 and c-C_3D_2/c-C_3HD ratios are very similar to those in dark clouds (Table 7), in spite of the different mechanisms thought to govern the abundances of unsaturated carbon chains and carbenes in these regions. In addition to the ion-molecule processes that produce carbon chains and carbenes in prestellar cores and cold dark clouds, sublimation of methane from grain mantles warmed up by the faint protostar is hypothesized to yield elevated abundances of carbon chains and carbenes in low-mass protostellar cores (see Cordiner et al. 2012, for a summary of the proposed mechanisms). Similar D/H ratios in prestellar and protostellar cores indicate that once the non-deuterated carbene is formed, the singly and doubly deuterated carbene are produced by reactions (2) to (5), notwithstanding the formation mechanism.

Table 7. Isomeric and D/H ratios of H_2CCC and c-C_3H_2 in six Galactic regions.

Property	Prestellar core		Protostellar core		Dark cloud	Translucent[a]	Diffuse[b]	PDR[c]
	TMC-1C	L1544	L1527[d]	Cha-MMS1[e]	TMC-1	(Average)	(Mean)	
$N(c\text{-}C_3H_2)$ cm^{-2}	$2.2^h \times 10^{13}$	$3.7^h \times 10^{13}$	1.3×10^{13}	2.7×10^{13}	$0.58^g \times 10^{14}$	2.4×10^{13}	3.3×10^{12}	9.3×10^{12}
$N(H_2CCC)$ cm^{-2}	$\mathbf{3.3 \times 10^{11}}$	$\mathbf{1.1 \times 10^{12}}$	1.1×10^{12}	···	$(2.1^g\text{-}\mathbf{3.1}) \times 10^{12}$	2.5×10^{12}	1.9×10^{11}	2.7×10^{12}
c-C_3H_2/H_2CCC	$\mathbf{67 \pm 7}^f$	$\mathbf{32 \pm 4}$	12	···	28 ± 6^g	9	17	3
c-C_3HD/c-C_3H_2	$(5\text{–}13)\%^h$ $10\%^i$	$(12\text{–}17)\%^h$ $15\%^{i,j}$	(7–18)%	(5–34)%	$8\%^i$ $5\%^k$	···	···	···
c-C_3D_2/c-C_3HD	$(3\text{–}15)\%^h$	$(7\text{–}17)\%^h$	$2.6\%^l$	···	···	···	···	···
$HDCCC/H_2CCC$	$\mathbf{19 \pm 5}\%$	$\mathbf{6 \pm 1.3}\%$	···	···	$\mathbf{4 \pm 1.6}\%$	···	···	···

Notes. Quantities in boldface are from this work.

References. [(a)] From Table 20 in Turner (2000) and references therein. [(b)] Liszt et al. (2012). [(c)] Pety et al. (2012). [(d)] From Table 1 in Sakai & Yamamoto (2013) and references therein. [(e)] Cordiner et al. (2012). [(f)] See Sects. 3.1 and 4. [(g)] Fossé et al. (2001). [(h)] Spezzano et al. (2013). [(i)] Bell et al. (1988). [(j)] Gerin et al. (1987). [(k)] See Table 12 in Turner (2001). [(l)] Tokudome et al. (2013).

A plausible explanation for the similar D/H ratios of c-C_3H_2 in the two types of dark cloud cores is as follows. Owing to freeze-out in the inner regions of prestellar cores – by analogy with the well-known case of HCO^+ and DCO^+, which are heavily depleted in the cold inner regions of prestellar cores – carbenes reside primarily in the warmer outer regions (Caselli 2002). As a result, if the abundance of H_2D^+ and the electron fraction in the outer regions of prestellar cores are similar to those in protostellar cores[7], according to reactions (2) to (5), similar c-C_3HD/c-C_3H_2 and c-C_3D_2/c-C_3HD ratios are expected. There are no observations of HDCCC in protostellar cores, but the next larger cumulene carbene HDCCCC has been detected in L1527 at ~3–4% that of H_2CCCC (Sakai et al. 2009b). Therefore, it would not be surprising if the $HDCCC/H_2CCC$ ratio in L1527 and other protostellar cores is similar to ratios in dense prestellar cores and dark clouds.

To gain a more conclusive understanding of the chemistry of the C_3H_2 system, the $HDCCC/H_2CCC$ and the c-C_3HD/c-C_3D_2 ratios should be systematically studied in a larger sample of dense cores. For example, Emprechtinger et al. (2009) have investigated the use of the N_2D^+/N_2H^+ ratio as an evolutionary tracer of Class 0 protostars. A comparison with the results obtained by Emprechtinger et al. (2009) would clarify whether the C_3H_2 system fails to be an evolutionary tracer, because carbenes are heavily depleted in the inner core of the cloud. Future observations with interferometers, NOEMA, and ALMA will shine some light on how the deuteration of different tracers changes with radial distance from the prestellar and protostellar core. More precise inferences derived from the observed D/H ratios in c-C_3H_2 and H_2CCC will also require further laboratory kinetic measurements. The reaction rates of the proton and deuteron transfer from H_3^+ (and deuterated isotopologues) to RH_2 (and deuterated isotopologues) have not been studied yet. Also the collisional rates for H_2CCC with H_2 are not yet available. The recombination of the linear and cyclic $C_3H_3^+$ with electrons has been studied by McLain et al. (2005) and Adams & Babcock (2005), but it cannot be confirmed that the skeleton of the ion is kept during the reaction. The deuteration of the C_3H_2 isomers will be better understood if the ionic intermediates, $C_3H_3^+$, $C_3H_2D^+$, $C_3HD_2^+$, and $C_3D_3^+$, were observed in dark clouds. Although laboratory-measured rotational spectra of these species are unavailable at present, high level quantum calculations for the $C_3H_3^+$ system are available to guide laboratory searches (Huang & Lee 2011). With precise laboratory rest frequencies in hand, deep radio astronomical searches for these ions could be undertaken, and the observed column densities (or upper limits) would allow refinements to chemical models of dark clouds.

Now that the rotational spectrum of HDCCC has been measured in the millimetre band and the molecule has been detected in three sources, a comprehensive kinetic model is needed to aid interpretation of the existing astronomical observations and to guide future observations of the C_3H_2 system. H_2CCC and c-C_3H_2 are currently considered separately in the KIDA chemical reaction database (Wakelam et al. 2015). However, to our knowledge, no complete model that distinguishes between the possibly different deuteration pathways for these two species currently exists. With the above caveats on missing laboratory data, we are working on a chemical model that includes the deuterated forms and spin states of these species, following the methods laid out in Sipilä et al. (2015). Observationally, several additional transitions should be measured in HDCCC, preferably in the centimetre band, thereby allowing a more accurate determination of the D/H ratio in H_2CCC. The $2_{0,2}$–$1_{0,1}$ transition at 38.77 GHz should be six times more intense, and the two $K_a = 1$ transitions at 38.28 and 39.25 GHz should be comparable to the line at 19.38 GHz. Unfortunately, it might not be feasible to observe the singly deuterated HDCCC in the less dense regions listed in Table 7, because the lines of H_2CCC are not very intense there. However, there are a number of cold dark clouds, prestellar cores, and protostellar cores in which HDCCC might be detectable, if the D/H ratio and the c-C_3H_2/H_2CCC isomeric ratio are comparable to those in TMC-1, TMC-1C, and L1544. These include L1527, Lupus-1, Lupus1-A, L483, ChaMMS1, and others where H_2CCC has been detected (Sakai et al. 2009b,a; Cordiner et al. 2012). Extending the determination of the D/H ratio in both isomers might serve as an independent test of models of dark cloud chemistry.

Acknowledgements. This work is carried out within the Collaborative Research Centre 956, sub-project [B2], funded by the Deutsche Forschungsgemeinschaft (DFG), and has also been supported by the NASA grant NNX13AE59G. S. Spezzano wishes to thank the Bonn Cologne Graduate School of Physics and Astronomy (BCGS) for financial support. Any opinions, findings, and conclusions in this article are those of the authors and do not necessarily reflect the views of the National Science Foundation.

References

Adams, N. G., & Babcock, L. M. 2005, J. Phys. Conf. Ser., 4, 38
Bell, M. B., Avery, L. W., Matthews, H. E., et al. 1988, ApJ, 326, 924

[7] This is indeed the case for low-mass cores in the Taurus complex, where Caselli et al. (2008) report similar column densities of ortho-H_2D^+ toward 5 prestellar and 2 protostellar cores: $N(\text{o-}H_2D^+) \sim 1\text{–}5 \times 10^{13}$ cm^{-2}. The electron fractions in the outer regions of typical low-mass cores as inferred from the DCO^+/HCO^+ and HCO^+/CO ratios are similar: $\sim 10^{-8}$–10^{-6} (Caselli 2002, and references therein).

Brünken, S., Gupta, H., Gottlieb, C. A., McCarthy, M. C., & Thaddeus, P. 2007, ApJ, 664, L43
Cernicharo, J., Guélin, M., Menten, K. M., & Walmsley, C. M. 1987, A&A, 181, L1
Cernicharo, J., Gottlieb, C. A., Guélin, M., et al. 1991, ApJ, 368, L39
Cernicharo, J., Cox, P., Fossé, D., & Güsten, R. 1999, A&A, 351, 341
Caselli, P. 2002, Planet. Space Sci., 50, 1133
Caselli, P., & Ceccarelli, C. 2012, A&ARv, 20, 56
Caselli, P., Vastel, C., Ceccarelli, C., van der Tak, F. F. S., & Bacmann, A. 2008, A&A, 492, 703
Chabot, M., Béroff, K., Gratier, P., Jallat, A., & Wakelam, V. 2013, ApJ, 771, 90
Cordiner, M., Charnley, S. B., Wirström, E. S., & Smith, R. G. 2012, ApJ, 744, 131
Cuadrado, S., Goicoechea, J. R., Pilleri, P., et al. 2015, A&A, 575, A82
Emprechtinger, M., Caselli, P., Volgenau, N. H., Stutzki, J., & Wiedner, M. C. 2009, A&A, 493, 89
Fossé, D., Cernicharo, J., Gerin, M., & Cox, P. 2001, ApJ, 552, 168
Gauss, J., & Stanton, J. F. 1999, J. Mol. Str., 485, 93
Gerin, M., Wootten, H. A., Combes, F., et al. 1987, A&A, 173, L1
Goldsmith, P. F., & Langer, W. D. 1999, ApJ, 517, 209
Gottlieb, C. A., Killian, T. C., Thaddeus, P., et al. 1993, J. Chem. Phys., 98, 4478
Huang, X., & Lee, T. J. 2011, ApJ, 736, 33
Kawaguchi, K., Kaifu, N., Ohishi, M., et al. 1991,PASJ, 43, 607
Kim, E., & Yamamoto, S. 2005, J. Mol. Spectr., 233, 93
Liszt, H., Sonnentrucker, P., Cordiner, M., & Gerin, M. 2012, ApJ, 753, L2
McLain, J. L., Poterya, V., Molek, C. D., et al. 2005, J. Phys. Chem. A, 109, 5119
Müller, H. S. P., Schlöder, F., Stutzki, J., & Winnewisser, G. 2005, J. Mol. Struct., 742, 215
Park, I. H., Wakelam, V., & Herbst, E. 2006, A&A, 449, 631
Pety, J., Teyssier, D., Fossé, D., et al. 2005, A&A, 435, 885
Pety, J., Gratier, P., Guzmán, V., et al. 2012, A&A, 548, A68
Sakai, N., & Yamamoto, S. 2013, Chem. Rev., 113, 8981
Sakai, N., Sakai, T., Hirota, T., Burton, M., & Yamamoto, S. 2009a, ApJ, 697, 769
Sakai, N., Sakai, T., Hirota, T., & Yamamoto, S. 2009b, ApJ, 702, 1025
Schöier, F. L., van der Tak, F. F. S., van Dishoeck, E. F., & Black, J. H. 2005, A&A, 432, 639
Sipilä, O., Caselli, P., & Harju, J. 2015, A&A, 578, A55
Spezzano, S., Tamassia, F., Thorwirth, S., et al. 2012, ApJS, 200, 1
Spezzano, S., Brünken, S., et al. 2013, ApJ, 769, L19
Talbi, D., & Herbst, E. 2001, A&A, 376, 663
Talbi, D., Hickman, A. P., Kashinski, D., Malenda, R. F., & Redondo, P. 2009, J. Phys. Conf. Ser., 192, 012014
Teyssier, D., Hily-Blant, P., Gerin, M., et al. 2005, ESA SP, 577, 423
Thaddeus, P., Gottlieb, C. A., Gupta, H., et al. 2008, ApJ, 677, 1132
Tokudome, T., Sakai, N., Sakai, T., Takano, S., & Yamamoto, S. 2013, ASP Conf. Ser., 476, 355
Troscompt, N., Faure, A., Maret, S., et al. 2009, A&A, 506, 1243
Turner, B. E. 2001, ApJS, 136, 579
Turner, B. E., Herbst, E., & Terzieva, R. 2000, ApJS, 126, 427
van der Tak, F. F. S., Black, J. H., Schöier, F. L., Jansen, D. J. M., & van Dishoeck, E. F. 2007, A&A, 468, 627
Vrtilek, J. M., Gottlieb, C. A., Gottlieb, E. W., Killian, T. C., & Thaddeus, P. 1990, ApJ, 364, L53
Wakelam, V., Loison, J.-C., Herbst, E., et al. 2015, ApJS, 217, 20
Ward-Thompson, D., Motte, F., & Andre, P. 1999, MNRAS, 305, 143
Wiesenfeld, L., & Faure, A. 2013, MNRAS, 432, 2573
Wu, Q., Hao, Q., Wilke, J. J., et al. 2010, J. Chem. Theory Comput., 6, 3122